Cell, Vol. 122, 941–945, September 23, 2005, Copyright ©2005 by Elsevier Inc. DOI 10.1016/j.cell.2005.07.004

Spiroplasma Swim by a Processive Change in Body Helicity

Joshua W. Shaevitz,[1,*] Joanna Y. Lee,[2] and Daniel A. Fletcher[3]
[1]Department of Integrative Biology
[2]Department of Plant and Microbial Biology
[3]Department of Bioengineering
University of California, Berkeley
459 Evans Hall
Berkeley, California 94720

Summary

Microscopic organisms must rely on very different strategies than their macroscopic counterparts to swim through liquid. To date, the best understood method for prokaryotic swimming employs the rotation of flagella. Here, we show that *Spiroplasma*, tiny helical bacteria that infect plants and insects, use a very different approach. By measuring cell kinematics during free swimming, we find that propulsion is generated by the propagation of kink pairs down the length of the cell body. A processive change in the helicity of the body creates these waves and enables directional movement.

Introduction

The ability to swim freely in liquids is a hallmark of many biological organisms. For large organisms such as fish, snakes, and humans, forward motion is achieved predominantly through the use of inertial forces (Childress, 1981; Veneti et al., 2005). However, for microorganisms, such as bacteria, the situation is very different. Inertial effects are small, so that a bacterium cannot rely on momentum, and movement is dominated by viscous forces. As a result, bacteria must swim using motions that are not time-symmetric in order to produce a net displacement (Ludwig, 1930; Purcell, 1977; Taylor, 1951). Many swimming bacteria, such as *Escherichia*, *Salmonella*, and spirochetes, satisfy this requirement by making use of rotary motion: they spin helical flagella located on the outside or inside of the cell body (Charon and Goldstein, 2002). However, non-flagellated bacteria, such as the mollicute *Spiroplasma* and the marine cyanobacterium *Synechococcus*, swim without the use of these large appendages (Waterbury et al., 1985; Whitcomb, 1980). The strategies that these organisms use to swim remain unclear.

Spiroplasmas, tiny gram-positive eubacteria that measure approximately 150 nm in width by a few microns in length, infect a wide range of plants and insects (Whitcomb, 1980 and references therein). They are unique among the wall-less bacteria of the class Mollicute in their ability to maintain a helical shape and swim in liquid media. *Spiroplasma*'s distinct morphology is defined by internal cytoskeletal filaments of a 55 kDa protein that assemble into a helical ribbon, termed the fibril ribbon (Townsend and Plaskitt, 1985; Trachtenberg and Gilad, 2001; Williamson et al., 1991). Recent results using cryo-electron tomography reveal a complicated intracellular organization involving the fibril ribbon as well as another helical structure, possibly the actin homolog MreB (Kurner et al., 2005).

In *Spiroplasma*, swimming is thought to arise from whole-cell undulations brought about by contractile motions of the cytoskeleton (Berg, 2002; Trachtenberg and Gilad, 2001; Wolgemuth et al., 2003). However, detailed kinematics of swimming has been difficult to observe due to the bacterium's minute size. Translation, rotation, and flexing of cells have all been reported (Daniels et al., 1980; Davis and Worley, 1973; Gilad et al., 2003), and cells are known to exhibit chemotaxis and viscotaxis, the ability to swim up or down gradients in chemical concentration or viscosity, respectively (Daniels et al., 1980). Chemotaxis most likely supplies *Spiroplasmas* with a selective advantage over other nonmotile organisms, although motility does not appear to be required for transmissibility and phytopathogenicity in at least one species of *Spiroplasma* (Bove et al., 2003).

Many aspects of *Spiroplasma* motility have been compared to the motions of another group of helical bacteria, the spirochetes (Whitcomb, 1980). Swimming in spirochetes is achieved by coupling internal periplasmic flagellar rotation to cell bending, twisting, rotation, and translation (Berg, 1976; Berg et al., 1978). During chemotaxis, flexing of the cell body about its midpoint is used to alter the swimming course for some spirochetes (Charon et al., 1992). Using this framework, it was proposed that rotation and flexing in *Spiroplasma* might serve these same purposes (Daniels et al., 1980; Gilad et al., 2003; Whitcomb, 1980). Here, we report the result of high-resolution video microscopy studies of swimming *Spiroplasma* cells. These data show that *Spiroplasma* swimming is driven by the propagation of a pair of kinks along the cell body and that these kinks are generated by a processive change in body helicity.

Results

Swimming Is Achieved through the Propagation of a Pair of Kinks in the Cell Body

To address the role of morphological changes in cell motility, we used differential interference contrast microscopy to analyze the motion of freely swimming *Spiroplasma melliferum* cells in liquid media. In stark contrast to spirochete motility, *Spiroplasma* swimming appears to be driven by the propagation of a pair of large kinks along the body axis of the cell. This method of propulsion generates thrust similarly to a wave of lateral displacement that travels down the length of a long, continuous cylinder from front to rear. Fluid coupled to the cell body moves rearward with the wave, propelling the bacterium forward (Taylor, 1951). Overall, cells moved in a zigzag path. As a kink progressed from one end of the *Spiroplasma* to the other, the viscous

*Correspondence: jshaevitz@berkeley.edu

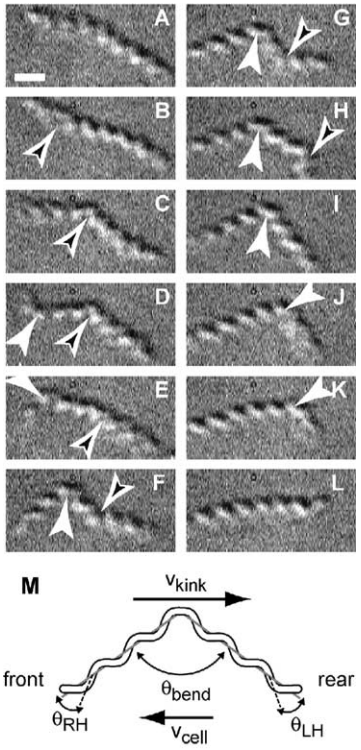

Figure 1. Kink Propagation along the Body Axis Occurs from Front to Rear during Swimming

(A–L) Selected video frames of a single swimming *Spiroplasma* cell, showing two propagating kinks taken at 0, 33, 132, 198, 297, 396, 429, 528, 627, 726, 792, and 858 ms. The first kink (black arrow) appears in (B) and moves to the right until reaching the rear of the body in (H). A second kink (white arrow) appears in (D) and leaves in (K). A change in chirality between the two sides of a kink can be seen in (G) and (I). Note that the cell rotates around its major axis between frames (B) and (C), (D) and (E), and (K) and (L). (M) Geometry of a kinked *Spiroplasma*. In the absence of strain, the kink angle, θ_{bend}, can be related to the two pitch angles θ_{RH} and θ_{LH} (see text). Propagation of the kink to the right at velocity v_{kink} propels the cell to the left at velocity v_{cell}. Scale bar, 1 μm.

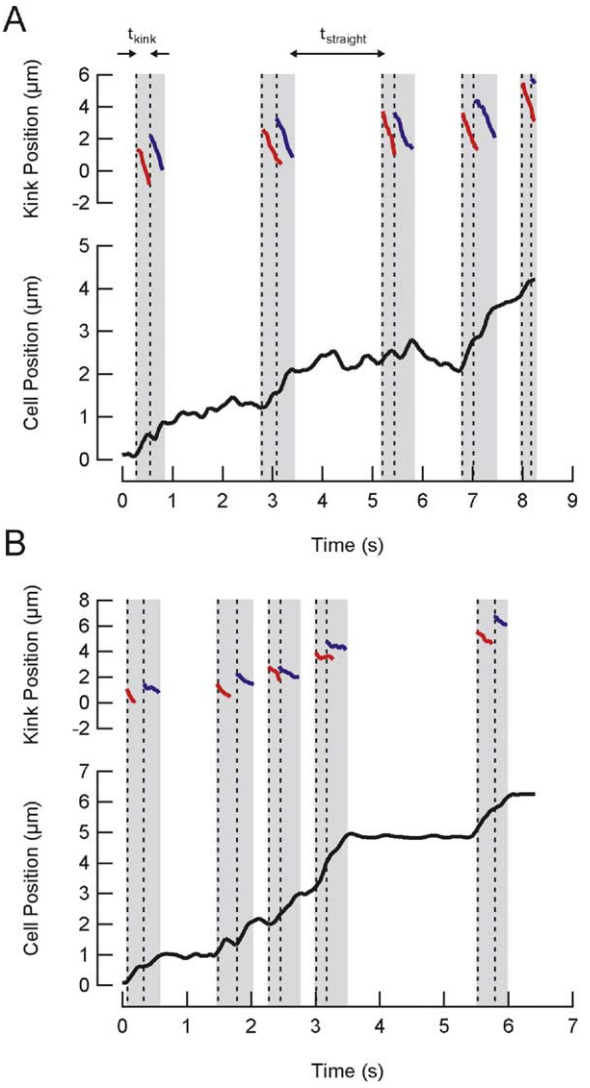

Figure 2. Representative Records of Cell and Kink Position against Time in Two Different Viscosities

The midpoint of a cell (solid black line) travels in the positive direction. Coming in pairs, kinks (red and blue lines) start at the front of the cell and propagate in the negative direction toward the rear. More Brownian motion and a lower propulsive efficiency are seen in the standard medium (A) than are seen in the medium with 0.5% methylcellulose (B). The start of each kink is denoted by a dotted line. Forward progress of the cell occurs primarily during kink motion (gray bars); the cells move very little between kink pairs. The time between kinks, t_{kink}, is typically much shorter than the time between kink pairs during which the cell is straight, $t_{straight}$. Records during which cell displacement occurred predominantly along one axis of the microscope were chosen such that a majority of the motion could be represented in a single trace. Cell positions were smoothed with a 175 ms boxcar filter for display.

drag on the largest kink-free portion of the body dominated, causing the cell to change direction by approximately the supplement of one bend angle (Figure 1).

Without exception, kinks started at the same end of the cell, which we operationally labeled as the front, and traveled smoothly toward the other end, the rear. It is unclear what structurally defines the front of a cell. Electron micrographs of *Spiroplasmas* with a tapered and a bulbous end have been reported (Ammar et al., 2004), but these differences cannot be resolved in our images due to the limited resolution of optical microscopy. Occasionally, a short-lived kink would appear at the rear of a cell. However, these kinks did not travel processively down the cell body and did not appear to interfere with kink creation at the front. In addition, cells tethered to a surface (which were not included in our analysis of swimming cells) often exhibited haphazard kinking. For these cells, kinks sometimes reflected off the point of surface attachment, reversing direction.

Kinks propagating along the cell body came in pairs (Figure 2). The distribution of times between kinks within a pair, t_{kink}, was approximately Gaussian with a mean of 0.26 s (Figure 3A). On average, the second kink was created at the front of the cell as the first neared the rear. In contrast, the time between kink pairs, during which the body remains straight, $t_{straight}$, appeared to be exponentially distributed with a time constant of 1 s (Figure 3B).

To ensure that the observed behavior represented

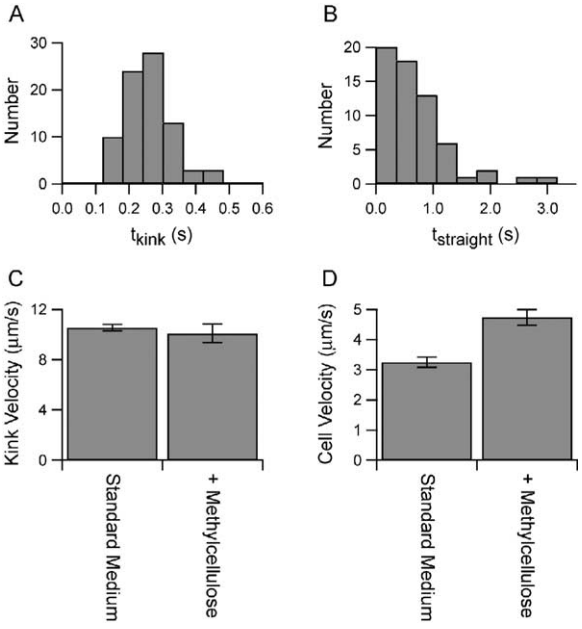

Figure 3. Distributions of Cell Swimming Parameters

(A) Histogram of the time between the beginning of each kink within a pair as defined in Figure 2. The time between kinks is Gaussian distributed with a mean of 0.26 ± 0.07 s (SD). (B) Histogram of the time when the cell is straight between kink pairs as defined in Figure 2. In contrast to the precise timing of the kinks within a pair, the distribution of $t_{straight}$ is wide and roughly exponential with a time constant of 0.9 ± 0.2 s (mean ± SEM). The addition of 0.5% methylcellulose (w/v) does not affect the velocity of kink propagation along the cell body (C), but it increases the efficiency of propulsion and thus the cell velocity during kink propagation (D). Error bars represent SEM.

free swimming, control experiments were performed in 70 μm thick flow chambers (data not shown). Swimming behavior in these cells was identical to those in the thinner slide preparations (see Experimental Procedures), although they swam more quickly out of the plane of focus.

Kinks Are Generated by a Change in Helicity

Kink location along the cell body corresponded to the position of a transformation in helicity (Figures 1G and 1I), reminiscent of kinks seen in mixed helices of flagella from *Salmonella* (Davis, 1978; Hotani, 1976). The helicity of a section of a cell can be deduced from the direction of slant of portions of that cell relative to the helical axis in an image focused above or below the cell (Goldstein and Charon, 1990; Matsuura et al., 1978; Shimada et al., 1975; Trachtenberg et al., 2003). To address whether this helical transformation is sufficient to explain the bend in the cell body, we measured the bend angle from each kink as well as the helical pitch angles at positions in front of and behind the kink (Figure 1M). Bend angles from all cells were remarkably constant and measured 111 ± 9 degrees (mean ± SD). If no strain is maintained at the junction between two cotangent, conormal helices, the bend angle is given by

$$\theta_{bend} = 180^\circ - \theta_1 - \theta_2,$$

where $\theta_{1,2}$ refer to the pitch angles of the helical section closer to the front or the back, respectively (Goldstein et al., 2000; Hotani, 1976). For *Spiroplasma*, we found that $\theta_1 = 34.6 \pm 0.5$ degrees, and $\theta_2 = 35.1 \pm 0.5$ degrees (mean ± SEM), which predicts a mean bend angle of 110 degrees, in excellent agreement with our measured value of 111 degrees. Our data are thus consistent with a model in which a kink is generated by the change in helicity, with no additional strain introduced into the system. Propagation of a kink is therefore created by a processive change in the helicity of the cell body from front to back.

Cells often rotated during kink propagation, a requirement for a helical transformation, although overall body rotation was loosely coupled to kink position and forward motion (Figure 1). Two forms of rotation satisfy this constraint (Goldstein et al., 2000): "crankshafting," in which one helical section rigidly pivots about the axis of the other, and "speedometer cable motion," where each helix rotates about its own axis. Swimming *Spiroplasma* cells exhibited both forms, although the latter appeared predominantly.

The observation that kinks come in pairs indicates that one handedness of the body helix is preferred. Due to an ambiguity in the position of the focal plane relative to a swimming cell, it is impossible for us to measure the absolute handedness of swimming cells. Traditionally, helicity is reconstructed from microscope images by moving the objective, or, equivalently, the microscope sample, such that an immobilized object of interest is examined at positions above and below the image plane. However, the Brownian motion of freely swimming cells is sufficiently large when compared to the depth of field of our microscope that we are unable to perform such a procedure. During our measurements, it is impossible to tell whether a freely swimming cell lies above or below the image plane. However, when viewed in electron micrographs, *Spiroplasma* are predominantly right-handed (RH) helices (Ammar et al., 2004; Davis and Worley, 1973; Townsend et al., 1980). On the basis of this observation, we assigned a RH chirality to cells measured in the straight phase (Figure 2). The appearance of the first kink in a pair, therefore, introduces a left-handed (LH) chirality, while the appearance of the second kink returns the cell to its normal RH chirality. Using this framework, we measured the pitch angles for the RH and LH helices and found them to be significantly different: $\theta_{RH} = 36.5 \pm 0.5$ degrees and $\theta_{LH} = 33.0 \pm 0.4$ degrees ($p < 10^{-6}$). This variation is similar to the difference between LH and RH flagellar filaments from *Salmonella*, which has been shown to arise from a change in the spacing of the flagellar subunits (Hotani, 1976; Macnab and Ornston, 1977). Similarly, we expect that the observed difference between the pitch angles for the two helicities seen in *Spiroplasma* cells is directly related to different configurations of the internal cytoskeleton.

Methylcellulose Increases Propulsive Efficiency and Cell Speed

The addition of methylcellulose caused cell speed to increase (Figure 2), in agreement with previous results on the effects of increased viscosity on *Spiroplasma* motility (Daniels et al., 1980; Davis, 1978; Gilad et al.,

2003). In standard medium, kinks moved along the cell body at a speed of 10.5 ± 0.3 μm/s relative to the front of the cell, and cells traveled at a velocity of 3.3 ± 0.2 μm/s in the direction opposite to that of the kink movement. The addition of 0.5% methylcellulose (w/v) to the medium did not affect the velocity of kink travel along the cell, but significantly increased the conversion of kink motion to forward movement (Figures 3C and 3D). In this solution, kinks traveled at a speed of 10.1 ± 0.7 μm/s, and cells swam with a velocity of 4.7 ± 0.3 μm/s. This increase in speed in the presence of methylcellulose, 42% for *Spiroplasma* cells, is also exhibited by spirochetes due to the gel-like character of this solution. A highly structured mesh of unbranched polymers, such as methylcellulose, forms a rigid network that is able to exert forces normal to a segment of the cell body even when that segment does not move in the normal direction (Berg and Turner, 1979).

Discussion

If unidirectional propagation of kinks is used for propulsion, how might *Spiroplasma* achieve chemotaxis? We expect that a directional bias is realized by modifying the time between kink pairs, using rotational Brownian motion to randomize the swimming course. This is similar to the strategy used by some bacteria whose flagellar motors only rotate in one direction (Armitage and Macnab, 1987; Chernova et al., 2003). If the dwell time between kink pairs is decreased in the presence of an increasing gradient of chemoattractant, cells swimming would become biased (Schnitzer et al., 1990). This model assumes that kinks occur and propagate faster than the rotational diffusion time of a *Spiroplasma* about a direction normal to the helical axis. Our cells measured 4.4 ± 0.8 μm long (mean ± SD), corresponding to a time of 6 s to diffuse about 60 degrees in 0.5% methylcellulose. Because the time spent kinked, about 0.6 s for a kink pair, is much less than the diffusion time, modulation of $t_{straight}$ can lead to chemotaxis.

Swimming on a microscopic scale can only be accomplished by a series of motions that are nonreciprocal, i.e., asymmetric with respect to time (Ludwig, 1930; Purcell, 1977; Taylor, 1951). Until now, bacterial swimming has been understood in terms of rotary motion exemplified in the form of flagellar spinning. Our data show that *Spiroplasma* propulsion, in contrast, is generated by waves of lateral displacement that propagate down the length of the cell, an entirely different mechanism. These waves are created by a change in the handedness of the cell body that naturally generates a 111 degree bend due to the pitch angles of right- and left-handed cells.

On the basis of these findings, it seems likely that the helical cytoskeleton of *Spiroplasma* can exist in two different states of helicity and that swimming takes advantage of this bistability. Theoretically, the energetics of helical transformations propagating along bistable helices has been shown to give rise to a variety of rotational motions, an analysis that should apply to *Spiroplasma* motility (Goldstein et al., 2000). The existence of a cell front from which kinks begin and the regular spacing in time of the two kinks within a pair provide strong evidence for the presence of a motor that initiates kink propagation. Further experiments will be necessary to provide details of this motor's structure and how it interacts with *Spiroplasma*'s dynamic cytoskeleton to produce motion.

Experimental Procedures

Culture and Culture Medium

Spiroplasma melliferum BC-3 (ATCC 33219) cells were grown at 32°C in T medium as described (Daniels et al., 1980).

Microscopic Observations

Active, exponentially growing *Spiroplasma* cultures were mixed with T medium, or T medium with 0.5% (w/v) methylcellulose (4,000 cps). Drops (2 μl) of these solutions were placed on microscope slides and covered with coverslips, and the edges were sealed with a Vaseline:lanolin:paraffin mixture (1:1:1) to prevent evaporation. Control experiments in larger flow chambers were performed by separating a coverslip from a glass slide by two pieces of 70 μm thick double-sided tape to form a channel through which cells in medium were added.

Observations were performed at room temperature on a modified Zeiss Axiovert S100 inverted microscope equipped with a 100W Hg arc lamp, a 100× 1.3 NA DIC objective, and a 1.4 N.A. DIC condenser. Images from the camera port were further magnified onto an NTSC CCD camera (Watec Co., Ltd., Japan) such that each camera pixel spanned a 37 nm × 37 nm square in the object plane. Video frames were digitized with a PCI bus frame grabber (National Instruments Corp., Austin, Texas) and streamed to hard disk via custom software written in Labview (National Instruments Corp., Austin, Texas). Movies of swimming cells were recorded for a minimum of 5 s up to a maximum of 45 s before cells would typically swim out of the field of view or plane of focus.

Image analysis of each movie frame was performed using custom software written in Igor Pro (Wavemetrics, Lake Oswego, Oregon). Morphological parameters and cell and kink velocities were measured for each swimming cell (standard medium, n = 11; 0.5% methylcellulose, n = 4). All measurements are reported as the mean ± SEM, unless otherwise noted.

Acknowledgments

We thank George Oster, Andrew Spakowitz, Steven Block, and the Fletcher lab for helpful discussions and careful reading of the manuscript. This work was supported by the Miller Institute for Basic Research in Science and an NSF CAREER Award to D.A.F.

Received: May 9, 2005
Revised: June 19, 2005
Accepted: July 8, 2005
Published: September 22, 2005

References

Ammar, E.-D., Fulton, D., Bai, X., Meulia, T., and Hogenhout, S.A. (2004). An attachment tip and pili-like structures in insect- and plant-pathogenic spiroplasmas of the class mollicutes. Arch. Microbiol. *181*, 97–105.

Armitage, J.P., and Macnab, R.M. (1987). Unidirectional, intermittent rotation of the flagellum of rhodobacter-sphaeroides. J. Bacteriol. *169*, 514–518.

Berg, H.C. (1976). How spirochetes may swim. J. Theor. Biol. *56*, 269–273.

Berg, H.C. (2002). How spiroplasma might swim. J. Bacteriol. *184*, 2063–2064.

Berg, H.C., and Turner, L. (1979). Movement of microorganisms in viscous environments. Nature *278*, 349–351.

Berg, H.C., Bromley, D.B., and Charon, N.W. (1978). Leptospiral motility. In Microbes in the Natural Environments, Symposia of the So-

ciety for General Microbiology, Volume 34 (Cambridge, UK: Cambridge University Press), pp. 285–295.

Bove, J.M., Renaudin, J., Saillard, C., Foissac, X., and Garnier, M. (2003). Spiroplasma citri, a plant pathogenic mollicute: Relationships with its two hosts, the plant and the leafhopper vector. Annu. Rev. Phytopathol. *41*, 483–500.

Charon, N.W., and Goldstein, S.F. (2002). Genetics of motility and chemotaxis of a fascinating group of bacteria: The spirochetes. Annu. Rev. Genet. *36*, 47–73.

Charon, N.W., Greenberg, E.P., Koopman, M.B., and Limberger, R.J. (1992). Spirochete chemotaxis, motility, and the structure of the spirochetal periplasmic flagella. Res. Microbiol. *143*, 597–603.

Chernova, A.A., Armitage, J.P., Packer, H.L., and Maini, P.K. (2003). Response kinetics of tethered bacteria to stepwise changes in nutrient concentration. Biosystems *71*, 51–59.

Childress, S. (1981). Mechanics of swimming and flying (Cambridge, England: Cambridge University Press).

Daniels, M.J., Longland, J.M., and Gilbart, J. (1980). Aspects of motility and chemotaxis in spiroplasmas. J. Gen. Microbiol. *118*, 429–436.

Davis, R.E. (1978). Spiroplasma associated with flowers of the tulip tree (Liriodendron tulipifera L.). Can. J. Microbiol. *24*, 954–959.

Davis, R.E., and Worley, J.F. (1973). Spiroplasma: Motile, helical microorganism associated with corn stunt disease. Phytopathology *63*, 403–408.

Gilad, R., Porat, A., and Trachtenberg, S. (2003). Motility modes of spiroplasma melliferum bc3: A helical, wall-less bacterium driven by a linear motor. Mol. Microbiol. *47*, 657–669.

Goldstein, R.E., Goriely, A., Huber, G., and Wolgemuth, C.W. (2000). Bistable helices. Phys. Rev. Lett. *84*, 1631–1634.

Goldstein, S.F., and Charon, N.W. (1990). Multiple-exposure photographic analysis of a motile spirochete. Proc. Natl. Acad. Sci. USA *87*, 4895–4899.

Hotani, H. (1976). Light microscope study of mixed helices in reconstituted Salmonella flagella. J. Mol. Biol. *106*, 151–166.

Kurner, J., Frangakis, A.S., and Baumeister, W. (2005). Cryo-electron tomography reveals the cytoskeletal structure of spiroplasma melliferum. Science *307*, 436–438.

Ludwig, W. (1930). Z. Vgl. Physiol. *13*, 397–504.

Macnab, R.M., and Ornston, M.K. (1977). Normal-to-curly flagellar transitions and their role in bacterial tumbling. Stabilization of an alternative quaternary structure by mechanical force. J. Mol. Biol. *112*, 1–30.

Matsuura, S., Kamiya, R., and Asakura, S. (1978). Transformation of straight flagella and recovery of motility in a mutant Escherichia coli. J. Mol. Biol. *118*, 431–440.

Purcell, E.M. (1977). Life at low Reynolds number. Am. J. Phys. *45*, 3–11.

Schnitzer, M.J., Block, S.M., Berg, H.C., and Purcell, E.M. (1990). Strategies for chemotaxis. In Biology of the Chemotactic Response, Symposia of the Society for General Microbiology, Volume 46 (Cambridge, UK: Cambridge University Press), pp. 15–34.

Shimada, K., Kamiya, R., and Asakura, S. (1975). Left-handed to right-handed helix conversion in Salmonella flagella. Nature *254*, 332–334.

Taylor, G. (1951). Analysis of the swimming of microscopic organisms. Proc. R. Soc. Lond. Ser. A *209*, 447–461.

Townsend, R., and Plaskitt, K.A. (1985). Immunogold localization of p55-fibril protein and p25-spiralin in spiroplasma cells. J. Gen. Microbiol. *131*, 983–992.

Townsend, R., Burgess, J., and Plaskitt, K.A. (1980). Morphology and ultrastructure of helical and nonhelical strains of spiroplasma citri. J. Bacteriol. *142*, 973–981.

Trachtenberg, S., and Gilad, R. (2001). A bacterial linear motor: Cellular and molecular organization of the contractile cytoskeleton of the helical bacterium spiroplasma melliferum bc3. Mol. Microbiol. *41*, 827–848.

Trachtenberg, S., Gilad, R., and Geffen, N. (2003). The bacterial linear motor of spiroplasma melliferum bc3: From single molecules to swimming cells. Mol. Microbiol. *47*, 671–697.

Veneti, Z., Bentley, J.K., Koana, T., Braig, H.R., and Hurst, G.D. (2005). A functional dosage compensation complex required for male killing in Drosophila. Science *307*, 1461–1463.

Waterbury, J.B., Willey, J.M., Franks, D.G., Valois, F.W., and Watson, S.W. (1985). A cyanobacterium capable of swimming motility. Science *230*, 74–76.

Whitcomb, R.F. (1980). The genus Spiroplasma. Annu. Rev. Microbiol. *34*, 677–709.

Williamson, D.L., Renaudin, J., and Bove, J.M. (1991). Nucleotide sequence of the spiroplasma citri fibril protein gene. J. Bacteriol. *173*, 4353–4362.

Wolgemuth, C.W., Igoshin, O., and Oster, G. (2003). The motility of mollicutes. Biophys. J. *85*, 828–842.